

Comitato Nazionale per l'Energia Nucleare  
ISTITUTO NAZIONALE DI FISICA NUCLEARE

Sottosezione di Firenze  
65/4

INFN/BE - 65/7  
26 Novembre 1965

M. Cevolani, G. Di Caporiacco and S. Petralia: ENERGY AND ANGULAR  
DISTRIBUTIONS OF  $\alpha$  PARTICLES IN THE  $^{20}\text{Ne}(n, \alpha)^{17}\text{O}$  REACTION  
AT 14 MeV. -

Reparto Tipografico  
dei Laboratori Nazionali di Frascati

340

INFN/BE-65/7  
26 Novembre 1965

M. Cevolani,<sup>(x)</sup> G. Di Caporiacco and S. Petralia<sup>(x)</sup>: ENERGY AND ANGULAR DISTRIBUTIONS OF  $\alpha$  PARTICLES IN THE  $^{20}\text{Ne}(n, \alpha)^{17}\text{O}$  REACTION AT 14 MeV<sup>(x)</sup>. -

ABSTRACT -

Energy and angular distributions for  $\alpha$  particles in the  $^{20}\text{Ne}(n, \alpha)^{17}\text{O}$  reaction have been obtained at  $E = 14.2$  MeV, by using a fast-cycle cloud chamber.

Departures from the typical evaporation distribution are observed in the low and high energy parts of the  $\alpha$  particles spectrum; the low energy part, however, is not especially significant owing to the distortion introduced by the  $(n, n\alpha)$  reaction. For the high energy  $\alpha$  particles the effect can be traced back to a direct interaction. In fact the angular distribution shows a distinct backward asymmetry (in the c. m. system) which becomes more pronounced for the more energetic  $\alpha$  particles. This peculiar feature, which is analogous with the reported results for the  $^{12}\text{C}(n, \alpha)^9\text{Be}$  and  $^{16}\text{O}(n, \alpha)^{13}\text{C}$  reactions, suggests that heavy particle stripping plays an important role also in the  $^{20}\text{Ne}(n, \alpha)^{17}\text{O}$  reaction.

1. INTRODUCTION -

In the study of nuclear reactions considerable effort is curren-

---

(x) - INFN, Sezione di Bologna.

(x) - This work has been performed as part of an Euratom-CNEN contract.

2.

tly being devoted to the separation of the so-called direct effect from the compound nucleus interactions.

The main source of experimental information for this purpose is given by angular distributions of the reaction products, which are expected to be symmetric around  $90^\circ$  in the c. m. system for a purely statistical mechanism, while they show more or less pronounced asymmetry for direct interactions.

Very few experimental investigations, however, have been devoted to angular distributions in  $(n, \alpha)$  reactions. Nevertheless some recent results show that there may be a special interest in this type of reaction, because there is some evidence, in the case  $^{12}\text{C}$  and  $^{16}\text{O}$ , that the distribution is peaked backwards<sup>(1, 2)</sup>. To account for it, a new type of direct reaction, namely heavy particle stripping, has been suggested.

It has been thought worthwhile, therefore, to investigate the  $^{20}\text{Ne}$   $(n, \alpha)$   $^{17}\text{O}$  reaction with 14.2 MeV neutrons by means of a cloud chamber. In fact, quite apart from the intrinsic phenomenological interest,  $^{20}\text{Ne}$  suggests itself as a nucleus, after  $^{12}\text{C}$  and  $^{16}\text{O}$ , which might be described in terms of  $\alpha$  particles clusters and might possibly supply further evidence for heavy particle stripping.

## 2. EXPERIMENTAL TECHNIQUE -

Neutrons were produced by a pulsed beam of deuterons which were accelerated to 360 KeV by a Cockcroft-Walton generator and made to impinge on a  $^3\text{H-Ti}$  target.

The recompression type cloud chamber was 20 cm in diam. and 7 cm in height; its centre was at 120 cm from the neutron source in a direction at  $90^\circ$  to the deuteron beam. The energy of the neutrons was therefore about 14.2 MeV.

The chamber was filled with pure Ne (99,9%) at 2 Atm. pressure; condensation was assured by water vapour only. Therefore, besides Ne, the only element present that could possibly give rise to spurious reactions was O.

Cloud chamber pictures were taken simultaneously with three cameras, which were placed at the vertices of an equilateral triangle, to allow easier stereoscopic reconstruction and check. Two distinct series were taken. In the first one, (1600 photograms), all visible events were measured, irrespective of the length of the tracks; an event was characterized by the typical fork of the emitted particle and recoil nucleus. For the second series, (1000 photograms), the scanning was speeded up by excluding the events for which none of the three simultaneous views showed  $\alpha$  tracks longer than 1 cm. This speedier procedure was adopted in order to enrich sub-

stantially the statistics for the lower lying levels of the residual nucleus and supplied, in any case, an unbiased statistics up to 8 MeV excitation energy of the residual nucleus.

As a whole over 10,000 events have been analyzed. The number of spurious events originated by diffused neutrons has been evaluated to be less than 6% of the total, by means of a third series of photograms which was taken for this purpose, after the cloud chamber, in the same position, had been suitably shielded from direct neutrons. Whenever possible and significant, the kinematic check on the two main series confirmed the above figure.

Spatial reconstruction of the tracks was carried out by means of IBM 650 computer, which also supplied the basic data, namely energy and angle of the particle in the c. m. system, the excitation energy of the residual nucleus and the weight to be assigned to the event in the statistics, to take the geometrical factors in due account (see later).

For events in which the residual excitation energy was less than 4,55 MeV the kinematic control was made; in this case the events were tentatively checked also for kinematic compatibility with other possible reactions, namely  $^{22}\text{Ne}(n, \alpha) ^{19}\text{O}$ ,  $^{20}\text{Ne}(n, p) ^{20}\text{F}$ ,  $^{16}\text{O}(n, \alpha) ^{13}\text{C}$ . Above 4,55 MeV this control is no more significant owing to the fact that  $^{17}\text{O}$  can deexcite by neutron emission.

The energy determination of the particles was made, in the hypothesis they were  $\alpha$  particles by means of the table of ranges given by Whaling(3).

The error in the energy measurement has been evaluated to 150 KeV on the basis of an uncertainty in the range equal to the average thickness of the track and taking also into account the errors in the pressure and the temperature of the gas in the cloud chamber.

The error in the measurement of the angles is a function of the length of the tracks and has been evaluated with reference to the ratio of the average thickness to the length of each track; it rarely exceeds  $2^\circ$  for the  $\alpha$  particles; for the recoil nucleus, however, the error is much larger and this produces sometimes a big uncertainty in the kinematical check.

The dimensions of the cloud chamber are of the same order of the most energetic particles emitted in the reactions; therefore, the distributions obtained directly from the observed tracks need corrections to take into account the probability of observing each individual event; a minor correction needs to be applied also to take into account the different probability of observing an event in the various points, owing to the different distance from the neutron source.

To evaluate this geometrical correction, first of all the useful zone of the chamber was determined, by noting the density of the start and

4.

end points of the observed tracks; this density has been found distinctly different from zero in a cylindrical zone 6 cm in height and 19 cm in diameter, while dropping fairly abruptly to zero outside. To make sure events were analyzed only if they were contained within a smaller internal region (5 cm height and 18 cm in diameter).

To these events a weight has been assigned, which is inversely proportional to the probability of production and observation. The probability of observation  $P_1$  depends only on the range  $R$  of the particle and on the angle  $\theta$  between the directions of the emitted particle and of the incoming neutron.

Let us call  $s$  (= 5 cm) and  $B$  (= 9 cm) the height and the radius of the useful volume of the chamber; then if  $R \sin \theta > s$ ,  $P_1$  is given by

$$P_1 = \frac{1}{\pi} \left( \operatorname{arctg} \frac{s}{\sqrt{R^2 \sin^2 \theta - s^2}} + \frac{1}{s} \sqrt{R^2 \sin^2 \theta - s^2} - \frac{R \sin \theta}{s} \right) .$$

(1)

$$\cdot \left( 4 \operatorname{arctg} \frac{\sqrt{4B^2 - R^2}}{R} - \frac{R}{B^2} \sqrt{4B^2 - R^2} \right)$$

while for  $R \sin \theta < s$  the first term within brackets is to be replaced by

$$(2) \quad \pi - \frac{R \sin \theta}{s}$$

The production probability  $P_2$  on the other hand, is inversely proportional to the square of  $L$ , the distance of the production point from the neutron source. In our case ( $L \gg B$ ) a simple and sufficiently accurate expression for  $P_2$  is:

$$(3) \quad P_2 = \frac{4D_1 D_2}{4D^2 + R^2 - 4DR \cos \theta}$$

where  $D_1$ ,  $D_2$  and  $D$  are respectively the distances from the neutron source of the farthest, the nearest and the central point of the chamber (see Appendix).

## 3. DISCUSSION OF POSSIBLE CONTAMINATIONS -

The only possible target nuclei in our chamber are  $^{20}\text{Ne}$ ,  $^{21}\text{Ne}$ ,  $^{22}\text{Ne}$ , and  $^{16}\text{O}$  (present in the water vapour); possible reactions with charged particle products are  $(n, \alpha)$ ,  $(n, \alpha n)$ ,  $(n, n\alpha)$ ,  $(n, p)$ ,  $(n, pn)$ ,  $(n, np)$  and, possibly, though with a probably small cross section,  $(n, d)$ . Reactions of the  $(n, \alpha n)$ ,  $(n, pn)$  type, as long as they can be considered two steps reactions (that is the neutron is emitted at a later time) need not to be separated from the  $(n, \alpha)$  and  $(n, p)$  reactions in energy and angular distributions;  $(n, n\alpha)$  reactions give  $\alpha$  particles of low energy which can be eliminated by suitably cutting the energy distribution. Hence the observed events belong necessarily to  $(n, \alpha)$  or  $(n, p)$  type on the above specified nuclei. Proton recoils from elastic scattering on Hydrogen are obviously excluded because in no case they can simulate the characteristic fork.

Simple visual inspection did not allow, in the operating conditions of our chamber, to distinguish with certainty in every case protons from alphas; nor was it always possible to separate  $(n, p)$  from  $(n, \alpha)$  reactions by kinematics; fortunately, however, it can be shown that the protons contribute at most 9% of the observed charged products. It was decided, therefore, to include in the energy and angular distributions all the events, evaluating them as if they were all  $(n, \alpha)$  reactions.

In fact, the size of our useful volume does not allow to record protons with more than 2.8 MeV energy; on the other hand protons with lower energy than 2.8 MeV are at most 25% of the total number of protons, as can be inferred from known proton spectra with  $(n, p)$  reactions in neighbouring nuclei<sup>(4)</sup>, while the whole  $(n, p)$  cross section is only about 1/3 of the corresponding  $(n, \alpha)$  cross section. This comes out from the calculations of Gardner<sup>(5)</sup> which gives  $\sigma(n, p) \simeq 100$  mb for  $^{20}\text{Ne}(n, p)^{20}\text{F}$  reaction and the inferred<sup>(6)</sup> value of  $\sigma(n, \alpha) \simeq 300$  mb for  $^{20}\text{Ne}(n, \alpha)^{17}\text{O}$  reaction.

The total proton contribution to the observed distribution of charged particles does not exceed, therefore, 9%. For the angular distribution we point out that in any case the low energy proton distribution is isotropic and cannot therefore be responsible for the observed anisotropy.

Finally we want to show that the observed energy and angular distributions as a whole can be legitimately assumed to represent essentially the  $^{20}\text{Ne}(n, \alpha)^{17}\text{O}$  reaction. In fact the total Oxygen mass in the chamber is about 2%; its cross section for the  $(n, \alpha)$  reaction at  $E_n = 14$  MeV is 300 mb, according to<sup>(7)</sup> while the  $(n, p)$  reaction has  $\sigma \simeq 90$  mb<sup>(8)</sup>. Since the reaction  $^{20}\text{Ne}(n, \alpha)^{17}\text{O}$  has also  $\sigma \simeq 300$  mb, as can be induced by the data of<sup>(6)</sup>, the oxygen contribution in our results comes out about 2%. The amount of  $^{21}\text{Ne}$  (and  $^{17}\text{O}$  and  $^{18}\text{O}$ ) is negligible;  $^{22}\text{Ne}$ , however, has a 8.8% abundance and no data are available on its cross sections; assuming, as a fair guess, a  $\sigma(n, \alpha)$  for  $^{22}\text{Ne}$  about half that of  $^{20}\text{Ne}$ , the events contributed by  $^{22}\text{Ne}$  would amount to less than 5%.

6.

In conclusion it can be safely assumed our distributions are due at least 85% to the  $^{20}\text{Ne} (n, \alpha) ^{17}\text{O}$  reactions, the next most likely contaminations coming, in order, from  $^{20}\text{Ne} (n, p)$ ,  $^{22}\text{Ne} (n, \alpha) ^{19}\text{O}$ , and  $^{16}\text{O} (n, \alpha) ^{12}\text{C}$ .

#### 4. ENERGY DISTRIBUTION -

The energy distribution, in the centre of mass system, of all the particles observed in the first series of photograms is shown in fig. 1. The maximum energy of 10,4 MeV nicely agree with the expected value of  $\alpha$  particles from the reaction  $^{20}\text{Ne} (n, \alpha) ^{17}\text{O}$  (whose Q is - 0,608 MeV). The maximum intensity in the distribution falls at 4,5 MeV, a reasonable value as compared to neighbour nuclei as  $^{23}\text{Ne}$  and  $^{27}\text{Al}(9)$  in view of the smaller Coulomb barrier of  $^{20}\text{Ne}$ . In the higher energy region the distribution shows a distinct departure from the maxwellian distribution, which would be expected from evaporative theory; of course, it is not surprising to find direct effects in this region and, in fact, we shall see that also the angular distribution leads to the same conclusion.

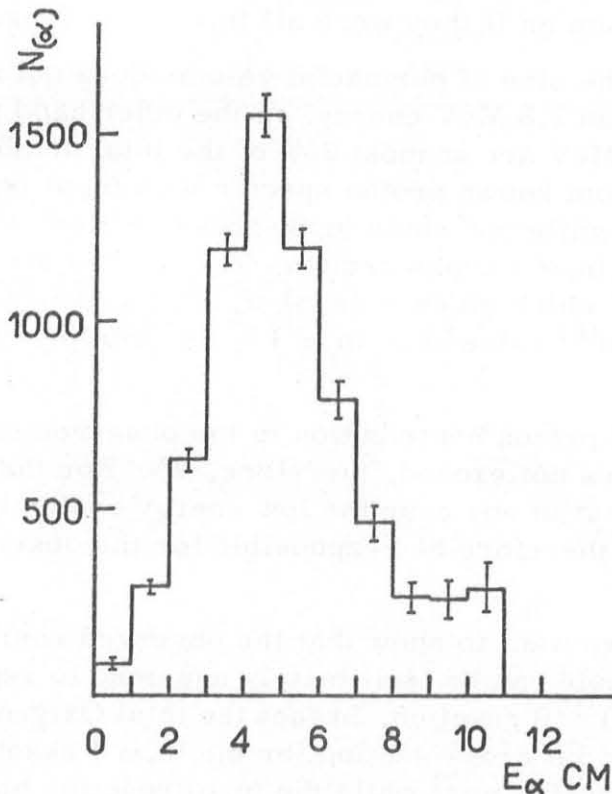


Fig. 1 - Energy distribution of the  $\alpha$  particles in the c. m. s.

The energy spectrum of the emitted particles ( $\alpha$  particles in our case) in the evaporative theory, is expressed by the classical formula<sup>(10)</sup> (Blatt and Weisskopf)

$$(4) \quad N(E_\alpha) dE_\alpha = \text{const } E_\alpha \sigma_c(E_\alpha) \rho(E_r) dE_\alpha$$

where  $E_\alpha$  is the energy of the particle,  $\sigma_c(E_\alpha)$  is the cross section for the compound nucleus formation (in the inverse reaction) and  $\rho(E_r)$  is the density of levels in the residual nucleus at the excitation energy  $E_r$ .

If we plot, as usual,  $\ln N(E_\alpha)/E_\alpha \sigma_c(E_\alpha)$  as a function of  $E_\alpha$  (instead of  $E_r$ ), by using for  $\sigma_c(E_\alpha)$  the values which can be obtained by extrapolation from Blatt and Weisskopf's tables<sup>(10)</sup> we get the diagram of fig. 2.

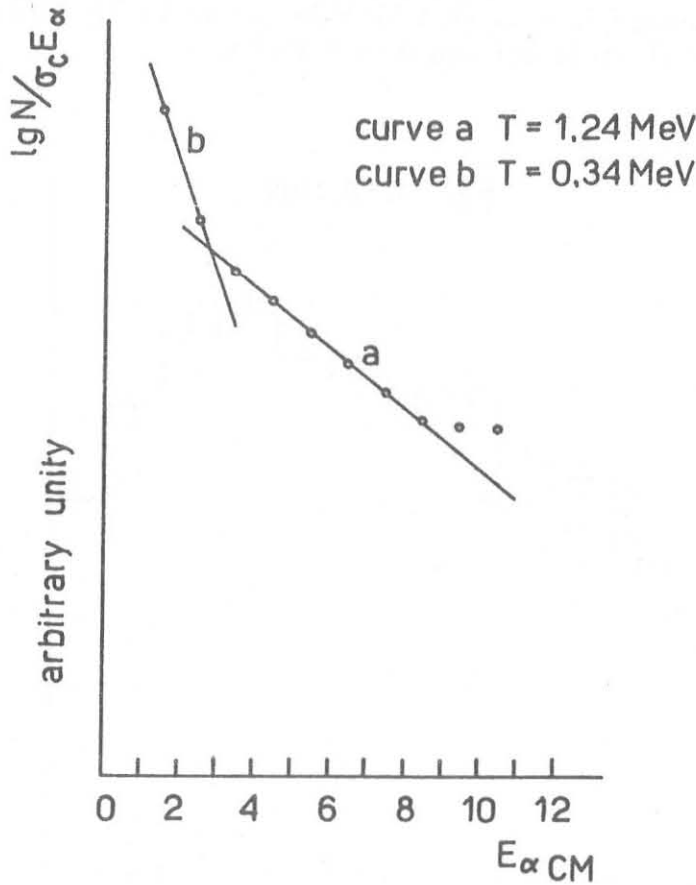


Fig. 2 - Plot of  $\ln [N(E_\alpha) / E_\alpha \sigma_c(E_\alpha)]$  versus  $E_\alpha$   
 a)  $T = 1,24$  MeV  
 b)  $T = 0,34$  MeV



8.

Three distinct parts are visible; for the purpose of deducing the "nuclear temperature" according to the well known formula

$$(5) \quad \zeta(E_r) = \text{const} \exp(E_r/T)$$

the high energy region has to be discarded owing to the presence of direct effects, as stated; the intermediate energy region  $E_\alpha = 3$  to 8 MeV gives a temperature of 1,24 MeV, while the low energy region would give a temperature of 0,34 MeV; this, however, is not surprising in view of the presence of  $(n, n\alpha)$  reactions, to which this part can reasonably be ascribed.

### 5. ANGULAR DISTRIBUTION -

The angular distribution in the c. m. system for all  $\alpha$  particles in the energy range 3.94 to 10.4 MeV is shown in fig. 3 (excitation energy of the residual nucleus from 0 to 8 MeV).

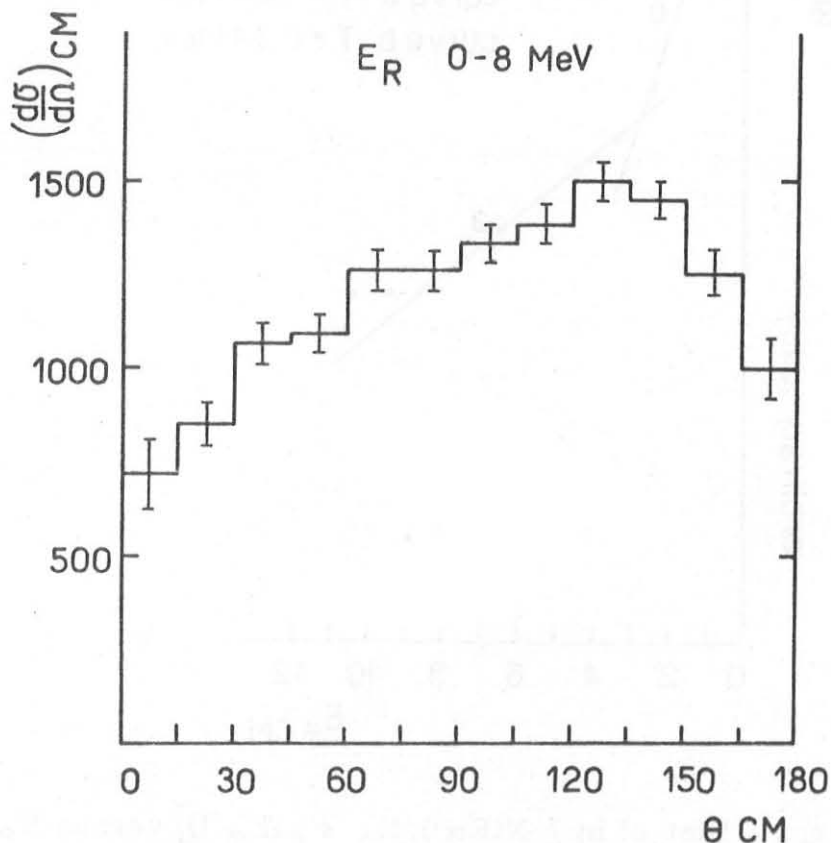


Fig. 3 - Angular distribution of the  $\alpha$  particles in the energy range from 3,94 to 10,4 MeV in the c. m. s.

For  $\theta = 0^\circ$  and  $\theta = 180^\circ$  the  $\alpha$  particle and the residual nucleus give tracks on the same line; the characteristic fork is not easily recognized in this case during the scanning; it is therefore possible that for the two extreme angular intervals  $0^\circ - 15^\circ$  and  $165^\circ - 180^\circ$  there has been some loss of real events, while the errors shown also for these classes are only the statistical ones.

Bearing this in mind the forward backward asymmetry was evaluated by taking the number of events  $n_f$  in which  $\alpha$  particles are emitted in the  $15^\circ - 90^\circ$  interval and the number of events  $n_b$  in the  $90^\circ - 165^\circ$  interval; we then define an asymmetry parameter  $s = \sqrt{2}(n_f - n_b)/(n_f + n_b)$  and we get  $s = -22\% \pm 3$ ; this backward asymmetry would be enhanced if the small, but unknown, isotropic contribution from protons could be subtracted.

The effect becomes even more pronounced if we take the angular distributions of the more energetic  $\alpha$  particles: the separate angular distributions for energy groups of the residual nucleus 0 to 3 MeV; 3 to 5 MeV; 5 to 7 MeV and 7 to 8 MeV are shown in fig. 4.

It is apparent that backward emission is strongly favoured in the 0-3 MeV ( $s = -38\% \pm 17$ ) and 3-5 MeV ( $s = -47\% \pm 9$ ) groups while for the interval 7-8 MeV the distribution appears to be symmetric with respect to  $90^\circ$  and more nearly isotropic.

We consider the effect in the interval 3 to 5 MeV as especially significant, because there is no reasonable doubt, in this interval, of possible contamination from other reactions.

This experimental picture is easily interpreted, at least qualitatively, if we consider it as an example of heavy particle stripping which seems, to date, the only mechanism capable to account for a prevailing backward emission.

This mechanism, suggested by Owen and Madansky<sup>(11)</sup> has been already invoked to account for similar angular distributions in the case of  $^{12}\text{C}(n,\alpha)^9\text{Be}$  and  $^{16}\text{O}(n,\alpha)^{13}\text{C}$  reactions. Our results, by supplying the new case of  $^{20}\text{Ne}(n,\alpha)^{17}\text{O}$ , give further evidence that this mechanism may be present at least in light nuclei. On the other hand, on a strictly experimental basis, we cannot completely exclude that the observed effect might have resulted from fluctuations of the Ericson type, the energy spread of the neutrons being only 0,2 MeV, that is of the same order of the expected correlation width for a light nucleus such as  $^{20}\text{Ne}$ .

The similarity of behaviour observed for  $^{12}\text{C}$ ,  $^{16}\text{O}$  and  $^{20}\text{Ne}$  seems however to favour the heavy particle stripping interpretation.

Further and more abundant data may be required to settle the question beyond any doubt.

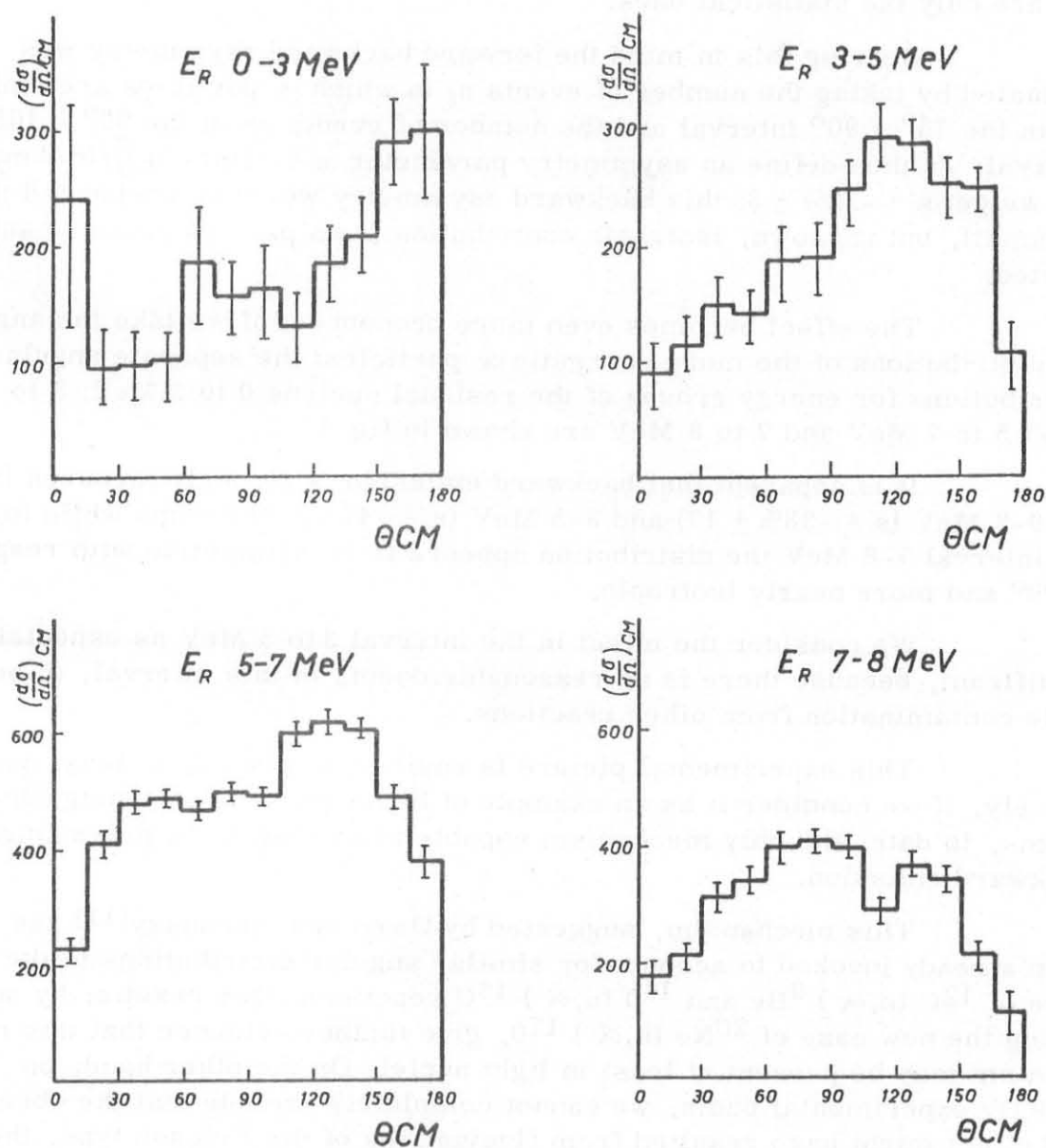
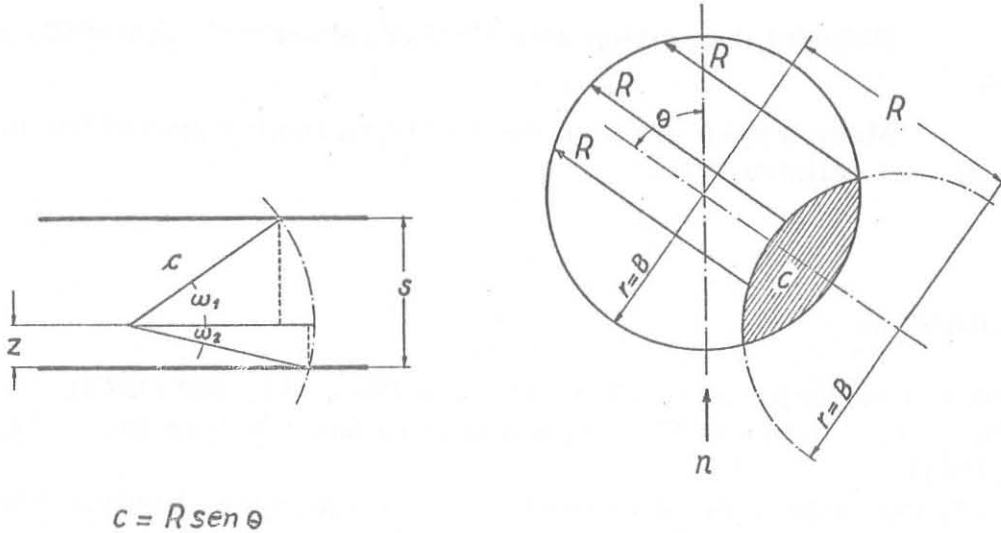


Fig. 4 - Angular distribution of the  $\alpha$  particles in the 0-3, 3-5, 5-7 and 7-8 MeV range of excitation energy of the residual nucleus  $^{170}\text{Lu}$ .

## APPENDIX -

Formula (1) can be derived as follows. The first factor in the right hand expression is equal to half the average fraction of total solid angle subtended by two parallel planes,  $s$  cm apart, from a point  $P$  between the planes, under the conditions that the intercept by the planes of every straight line through  $P$  forming an angle  $\theta$  with the direction of the incoming neutrons, has a distance from  $P$  bigger than  $R$ . This is with the notations of fig. 5.



$$c = R \text{ sen } \theta$$

Fig. 5 - Cloud chamber views for the range of the  $\alpha$  particles calculation.

$$\frac{1}{s} \int_0^s \frac{\omega_1 + \omega_2}{2\pi} dz = \frac{1}{2\pi s} \int_0^s \left( \arcsen \frac{s-z}{c} + \arcsen \frac{z}{c} \right) dz = \frac{1}{\pi} \left( \text{arctg} \frac{s}{\sqrt{c^2 - s^2}} + \frac{1}{s} \sqrt{c^2 - s^2} - \frac{c}{s} \right)$$

being  $c = R \text{ sen } \theta$

The second factor in formula (1) is the ratio of the surface, across the chamber, from which tracks with range  $R$  and angle  $\theta$  can still originate and be observed (ending in the chamber) and the total surface of the chamber.

Particles with angle of emission  $\theta$  and range  $R$  are obviously visible if their tracks originate in the field  $C$ , defined as the common surface of two circles with radius  $B$ , the centres of which are  $R$  cm apart.

This common area is

$$2B^2 \text{ arctg} \frac{\sqrt{4B^2 - R^2}}{R} - \frac{R}{2} \sqrt{4B^2 - R^2}$$

This has to be multiplied by 2, to take into account the two symmetric directions, which were not included in the solid angle in (1).

Finally in the formula (3) for the probability  $P_2$  the denominator is simply 4 times the square distance from the neutron source to the centre of the area C.

#### ACKNOWLEDGEMENTS -

Helpful discussion with Prof. M. Mandò are gratefully acknowledged.

Many thanks are also due to Mr. G. Degli Espositi for his skillful technical collaboration.

#### REFERENCES -

- (1) - M. L. Chatterjee and B. Sen, Nuclear Phys. 51, 583 (1964).
- (2) - N. Cindro, I. Slans, P. Tomas and B. Eman, Nuclear Phys. 22, 96 (1961).
- (3) - Whaling, Handbook of Physics, Vol. 34 (Springer, Berlin, 1958) p. 193
- (4) - R. N. Glover and K. H. Purser, Nuclear Phys. 24, 431, 630 (1961);  
D. L. Allan, Nuclear Phys. 10, 348 (1959);  
L. Colli et al. Nuovo Cimento 20, 928 (1961);  
L. Colli et al. Nuovo Cimento 21, 966 (1961).
- (5) - D. G. Gardner, Nuclear Phys. 29, 373 (1962).
- (6) - R. E. Shamu, Nuclear Phys. 31, 166 (1962).
- (7) - A. B. Lillie, Phys. Rev. 87, 716 (1952).
- (8) - H. C. Martin, Phys. Rev. 93, 498 (1954).
- (9) - P. G. Bizzetti, A. M. Bizzetti Sona, M. Bocciolini, Nuclear Phys. 36, 950 (1961);  
W. Patzak and M. Vonach, Nuclear Phys. 39, 263 (1962).
- (10) - J. M. Blatt and V. Weisskopf, Theoretical Nuclear Physics (Wiley, New York, 1952) p. 353.
- (11) - L. Madansky and G. E. Owen, Phys. Rev. 99, 1608 (1955); 105, 1766 (1957).